THE JOURNAL OF BIOLOGICAL CHEMISTRY VOL. 288, NO. 36, pp. 26323–26334, September 6, 2013

Metastasis Suppressor Tetraspanin CD82/KAI1 Regulates Ubiquitylation of Epidermal Growth Factor Receptor*[S]

Received for publication, July 10, 2013, and in revised form, July 25, 2013 Published, JBC Papers in Press, July 29, 2013, DOI 10.1074/jbc.M112.439380

Elena Odintsova[‡1], Guillaume van Niel[§], Hélène Conjeaud[¶], Graça Raposo[§], Ryo Iwamoto[‖], Eisuke Mekada[‖], and Fedor Berditchevski[‡]

From the [‡]School of Cancer Sciences, College of Medical and Dental Sciences, University of Birmingham, Birmingham B15 2TT, United Kingdom, the [§]Institut Curie, Centre de Recherche, and Unité Mixte de Recherche 144, Centre National de la Recherche Scientifique, F-75248 Paris, France, the [¶]Matière et Systèmes Complexes, UMR 7057 CNRS, Université Denis Diderot Paris-VII, 75205 Paris, France, and the [‖]Research Institute for Microbial Diseases, Osaka University, Osaka 565-0871, Japan

Background: Tetraspanin CD82/KAI1 is associated with EGF receptor and regulates its signaling.
Results: CD82 controls ubiquitylation of EGF receptor after stimulation with heparin-binding ligands and alters receptor trafficking.
Conclusion: CD82 regulates communication between heparan sulfate proteoglycans and ligand-bound EGFR, thus affecting the activity of c-Cbl.
Significance: Lateral cross-talk initiated by CD82-dependent interactions is critical for modulation of EGFR function.

Ligand-induced ubiquitylation of EGF receptor (EGFR) is an important regulatory mechanism that controls endocytic trafficking of the receptor and its signaling potential. Here we report that tetraspanin CD82/KAI1 specifically suppresses ubiquitylation of EGFR after stimulation with heparin-binding EGF or amphiregulin and alters the rate of recruitment of the activated receptor to EEA1-positive endosomes. The suppressive effect of CD82 is dependent on the heparin-binding domain of the ligand. Deletion of the C-terminal cytoplasmic domain of CD82 (CD82ΔC mutant) inhibits endocytic trafficking of the tetraspanin and compromises its activity toward heparin-binding EGF-activated EGFR. Reduced ubiquitylation of EGFR is accompanied by PKC-dependent increase in serine phosphorylation of c-Cbl in cells expressing elevated levels of CD82. Furthermore, phosphorylation of threonine 654 (PKC phosphorylation site) in the juxtamembrane domain of the receptor is considerably increased in CD82-expressing cells. These results describe previously unsuspected links between tetraspanin proteins and ubiquitylation of their molecular partners (*e.g.*, EGFR). Our data identify CD82 as a new regulator of c-Cbl, which discriminatively controls the activity of this E3 ubiquitin ligase toward heparin-binding ligand-EGFR pairs. Taken together, these observations provide an important new insight into the modulatory role of CD82 in endocytic trafficking of EGF receptor.

Tetraspanins comprise a family of four transmembrane domains proteins that function as the main structural components and organizers of specific microdomains: tetraspanin-enriched microdomains (TERM).[2] Within TERM, tetraspanins link together various receptors and cytoplasmic signaling molecules and regulate lateral cross-talk at the plasma membrane (1–3). In addition, there is growing evidence that tetraspanins have a role in trafficking, sorting in endosomes and exocytosis of the molecules associated with TERM (4). However, endocytic trafficking routes for the majority of tetraspanins and the molecular mechanisms underlying their role in endocytic trafficking of associated partners remain largely unknown.

Metastasis suppressor tetraspanin CD82/KAI1 has been implicated in the modulation of activities of various transmembrane receptors such as EGFR, c-Met, and β1 integrins (5–11). Specifically, we have previously shown that elevated expression of CD82 in epithelial cells results in the increased internalization rate of EGFR, thus attenuating the signaling of the receptor (5). A more recent report described the involvement of CD82 in controlling EGFR diffusion in the plasma membrane and its interaction with the machinery of clathrin-dependent endocytosis (12). Likewise, there is evidence that CD82 regulates surface levels of $\alpha6\beta1$ integrin by accelerating its ligand-dependent internalization (7). Previously described modulatory activities of CD82 were directed toward the cell surface pool of the associated receptors. Indeed, until recently, the intracellular distribution of CD82 has been studied mainly in hematopoetic cells, where it was shown to be abundant in multivesicular bodies in B lymphocytes (13) and in endolysosomal tubules in dendritic cells (14). In their recent report Xu *et al.* (15) confirmed that in prostate epithelial cells CD82 is localized to various endocytic organelles including late endosomes and lysosomes. They also showed that CD82 is internalized via clathrin- and dynamin-independent pathways (15). However, neither the intracellular pathways of internalized CD82 nor the

* This work was supported by Breast Cancer Campaign Grants 2008MaySP18, 2007PR22, and 2003:712 (to E. O. and F. B.).
[S] This article contains supplemental Fig. S1.
[1] To whom correspondence should be addressed: School of Cancer Sciences, College of Medical and Dental Sciences, University of Birmingham, Edgbaston, Birmingham B15 2TT, UK. Tel.: 44-121-4151043; Fax: 44-121-4144486; E-mail: e.odintsova@bham.ac.uk.

[2] The abbreviations used are: TERM, tetraspanin-enriched microdomain; EGFR, EGF receptor; HB-EGF, heparin-binding EGF; AR, amphiregulin; EEA1, early endosomal antigen 1; HSPG, heparan sulfate proteoglycans; PM, plasma membrane.

involvement of this tetraspanin in postendocytic trafficking of its associated proteins has been investigated in previous studies.

The level and duration of EGFR signaling is determined by a variety of factors, not the least by the post-translational modifications initiated by ligand binding (16). Different ligands induce diverse cellular responses and may result in different outcomes for the receptor (17).

In this study we have found that CD82 reduces the level of ubiquitylation of EGFR following stimulation with HB-EGF and AR. Heparin-binding domain of the ligand is essential for CD82-induced changes in the ubiquitylation of the receptor. Moreover, this correlates with delayed HB-EGF-induced phosphorylation of EGFR on Tyr^{1045}, the recruitment point for c-Cbl to the receptor. Changes in ubiquitylation may be correlated with the activation of PKC because phosphorylation of Thr^{654} on EGFR (main PKC phosphorylation site) is increased in CD82-expressing cells. Furthermore, increase in serine phosphorylation of c-Cbl is PKC-dependent in CD82-expressing cells. We also found that a reduced level of ubiquitylation of EGFR resulted in diversification of its postendocytic trafficking route. Specifically, we established that CD82 alters kinetics of the recruitment of ligand-stimulated receptor to early endosomes and egress from these compartments. Importantly, these activities of CD82 toward EGFR are dependent on the C-terminal cytoplasmic region of the tetraspanin. Thus, this study has established a new paradigm for tetraspanin-dependent regulation of postendocytic trafficking of their associated receptors.

EXPERIMENTAL PROCEDURES

Mutagenesis and Viral Transduction—The mutant of CD82 (CD82ΔC) with the last 11 amino acids (HSEDYSKVPKY) deleted for this study was generated by a standard PCR protocol (sequences of the primers are available upon request). Stable transfectants of HB2 cells with mutant and wild type CD82 were generated by using retroviral transduction. First, FLY A13 packaging cells were transfected with the plasmid containing appropriate cDNA by using Lipofectamine (Invitrogen) according to the manufacturer's protocol. Five days later, the medium was harvested for use as a "transient virus." Second, HB2 cells were infected overnight with various dilutions of virus. After 3 days, the puromycin selection was started. The puromycin-resistant colonies were pooled together and sorted by flow cytometry with an anti-CD82 mAb (IA4).

2.5.2A cells depleted of CD82 were generated using MISSION shRNA library (Sigma) following the manufacturer's protocol. Successful clones were selected in puromycin-containing medium.

Cell Lines, Antibodies, and Reagents—Human mammary epithelial cells HB2 and 2.5.2A (18) wild type cells were maintained in DMEM (Invitrogen) supplemented with 10% FCS, 10 μg/ml of hydrocortisone, and 10 μg/ml of insulin. HB2/CD82wt, HB2/CD82ΔC, and 2.5.2A/shCD82 (3) cells were propagated in the same medium supplemented with puromycin (2 μg/ml).

The anti-CD82 mAb M104 was kindly provided by Dr. O. Yoshie. The anti-CD82 mAb TS82b was kindly provided by Dr. E. Rubinstein. We are grateful to Professor M. Marsh for providing anti-CD63 mAb (1B5). Anti-EGFR mAbs (Ab-16, Ab-15, and Ab-12) were purchased from ThermoScientific (Lab Vision). Anti-c-Cbl polyclonal antibody was purchased from R&D Systems, and anti-c-Cbl mAb (A-9) was from Santa Cruz. Anti-phosphoserine polyclonal antibody was from Abcam. Anti-phospho-c-Cbl (Tyr^{774} and Tyr^{331}) and anti-phospho-EGFR (Tyr^{1068} and Tyr^{1045}) rabbit monoclonal antibodies were purchased from Cell Signaling Technology. Anti-phospho-EGFR (Thr^{654}) antibody (clone 3F2) was purchased from Millipore. Anti-EEA1 mAb was from Transduction Lab. Mono- and polyubiquitinylated conjugates, mouse mAb (clone FK2) was purchased from Enzo Life Sciences. All Alexa Fluor-conjugated secondary antibodies for immunofluorescence were purchased from Molecular Probes, Invitrogen/Life Sciences. IRDye800 or IRDye680 secondary antibodies were purchased from LI-COR Biosciences. The PKC inhibitor Calphostin C was purchased from R&D Systems. Other reagents were from Sigma or Thermo Fisher Scientific.

Co-immunoprecipitation of EGFR and c-Cbl and Ubiquitylation of EGFR—Cells were serum-starved overnight and incubated with the ligand in HEPES-supplemented DMEM for the indicated time intervals at 37 °C. After incubation, the cells were quickly washed with ice-cold PBS and lysed in buffer containing 1% Triton X-100, 2 mM phenylmethylsulfonyl fluoride, 10 μg/ml aprotinin, 10 μg/ml leupeptin, and phosphatase inhibitors (also supplemented with iodoacetomide (20 mM) if lysates were used for detection of ubiquitylated species) for 1.5 h at 4 °C. The insoluble material was pelleted at 7000 × *g* for 10 min. EGFR was immunoprecipitated with the Ab-12 (anti-EGFR mAb) for 2 h at 4 °C on the rotating wheel, and then the mixture was incubated with protein G-agarose beads for 2 h at 4 °C as before (19). The complexes were eluted from the beads with Laemmli loading buffer. Proteins were resolved in 10% SDS-PAGE, transferred to a nitrocellulose membrane, and developed with the appropriate antibody. Protein bands were visualized using horseradish peroxidase-conjugated goat anti-mouse antibodies (Dako) and chemiluminescence reagent (PerkinElmer Life Sciences) or IRDye800 secondary antibody for detection using the LI-COR Odyssey Imaging System. Production and purification of sΔHB-EGF has been described elsewhere (20, 21).

Detection of Phosphorylated Proteins—Detection of phosphorylated proteins was carried out by Western blotting. The cells were serum-starved overnight and, after incubation with the ligand for indicated time intervals, were lysed with hot Laemmli buffer supplemented with inhibitor mixture as described above. Equal amounts of protein were resolved in 10% SDS-PAGE, transferred to a nitrocellulose membrane, and developed with phospho-specific antibodies.

Inhibitor Treatment—HB2 and HB2/CD82 cells were plated on 6-cm dishes 24 h before the start of the experiment. The cells were serum-starved overnight and treated with 5 μM Calphostin C for 1.5 h. Subsequent incubation with HB-EGF was carried out in the presence of the inhibitor. Appropriate concentration of the drug was determined in a pilot experiment.

Measurement of Changes in Surface Levels of EGFR by Flow Cytometry—The cells were incubated on ice with growth factors for 1 h, then washed, and transferred to 37 °C for the indicated time intervals. After incubation, they were quickly transferred to ice, washed with ice-cold PBS, detached on ice with

EDTA, incubated with primary antibodies for 45 min on ice, washed twice with wash buffer (0.1% heat-inactivated BSA/PBS), and then labeled with FITC-conjugated goat anti-mouse IgG for 45 min on ice. After two washes, the cells were fixed with 2% paraformaldehyde and analyzed using Coulter Epics program (Becton Dickinson).

Immunofluorescence—The cells were grown on glass coverslips in complete medium for 24–36 h, serum-starved overnight, and incubated with ligand (and/or mouse monoclonal antibody against CD82 (TS82b)) for the indicated time intervals. After incubation, the cells were fixed with 2% paraformaldehyde/PBS for 10 min and, if necessary, permeabilized with 0.1% Triton X-100/PBS for 2 min. Staining with primary and fluorochrome-conjugated secondary antibodies was carried out as previously described (22). The images were captured using Zeiss LSM510 META confocal system with 63× oil immersion objective (NA 1.4). Z-stack sections were collected at 0.3–0.4-μm intervals. Quantification of co-localization was carried out on 40–50 cells from two or three experiments using ImageJ Plugin JACOP (23).

Microplate Internalization Assay—The cells were plated on 96-well flat-bottomed plates at the density 5×10^3 cells/well, 6 wells for each time point. After 48 h, the cells were washed three times with ice-cold PBS and incubated with the primary antibody (anti-CD82 mAb, TS82b) at 4 °C for 1 h. Three washes with PBS were followed by incubation at 37 °C in full medium for various time intervals. Then cells were fixed with 2% paraformaldehyde for 10 min, blocked with 1% heat-inactivated BSA in PBS, and incubated with IRDye 800CW goat anti-mouse IgG from LI-COR Biosciences. After three washes with PBS, the plates were dried, and fluorescence was quantified in 800-nm channel by the Odyssey Infrared Imaging System (LI-COR Biosciences). Experiments were carried out at least three times. Statistical significance was calculated by paired, two-tailed *t* test.

Electron Microscopy—For immunoelectron microscopy, cells were fixed in 2% paraformaldehyde, 0.125% glutaraldehyde (Sigma-Aldrich) in 0.2 M phosphate buffer (pH 7.4) and recovered from the culture plates using cell scrapers. The cells were embedded in 10% gelatin and infused with 2.3 M sucrose as described previously (24, 25). Gelatin blocks were frozen in liquid nitrogen, and ultrathin sections were collected on drops containing a mixture of methylcellulose and sucrose (25), deposited on Formvar carbon-coated copper grids and single- or double-immunogold labeled using indicated antibodies and protein A coupled to 10- or 15-nm gold particles. Protein A-conjugated 10- or 15-nm gold particles (PAG10 or PAG15) were purchased from the microscopy center of Utrecht University (Utrecht, the Netherlands). Grids were contrasted/embedded in 0.4% uranyl acetate, 1.8% methylcellulose and dried. For conventional electron microscopy with pre-embedding labeling, cells grown on coverslips were incubated with anti-CD82 mAb (TS82b or IA4) at 4 °C for 1 h. After three washes (to remove unbound antibody), the cells were incubated with protein A coupled to 10-nm gold particles at 4 °C for 1 h. After three washes (to remove unbound gold particles), the cells were chased at 37 °C in full medium for the indicated time intervals. The cells were then fixed with 2.5% glutaraldehyde in 0.1 M cacodylate buffer for 90 min, post-fixed with 2% OsO4, dehydrated in ethanol, and embedded in Epon. Ultrathin (60–70 nm) sections were examined using a Philips CM120 electron microscope (FEI Company, Eindhoven, the Netherlands) equipped with a digital camera Keen View (OSIS, Münster, Germany).

RESULTS

HB-EGF-induced Ubiquitylation of EGFR Is Impaired in Cells with High Expression Level of CD82—EGF receptor signaling potential depends on a delicate balance between processes of recycling and degradation. The fate of the receptor is decided in sorting endosomes following ligand-induced internalization. One of the critical regulatory mechanisms of intracellular trafficking of the activated EGFR is ubiquitylation (17). Following earlier reports describing the role of CD82 in EGF-induced internalization of EGFR (5, 12), we investigated whether ligand-induced ubiquitylation of the receptor is influenced by this tetraspanin. We examined three ligands (EGF, AR, and HB-EGF) that are known to induce different levels of ubiquitylation and have distinct effects on the postendocytic trafficking of EGFR (26). Cells with low or high levels of CD82 (Fig. 1*A*) were serum-starved overnight, and kinetics of ubiquitylation of EGFR in response to the ligands were investigated after a chase with a ligand for up to 30 min at 37 °C. Stimulation of the control cells (HB2) with EGF and HB-EGF induced robust ubiquitylation of EGFR (Fig. 1, *B* and *C*, *lanes 1–5*), reaching the maximum at 5–15 min. Amphiregulin induced weaker ubiquitylation of the receptor with a maximum at 5 min (Fig. 1*D*, *lanes 1–5*). Weaker AR-induced ubiquitylation of EGFR was previously reported and linked to the initiation of higher recycling rate of AR-activated receptor (26, 27).) When the cells with high expression level of CD82 (HB2/CD82) were stimulated with EGF, we observed similar kinetics and degree of EGF-induced ubiquitylation of the receptor (Fig. 1*B*, *lanes 6–10*). By contrast, ubiquitylation of EGFR stimulated with either HB-EGF or AR was markedly impaired (2–3-fold, depending on ligand and time point) in HB2/CD82 cells when compared with control cells (Fig. 1, *C* and *D*, *lanes 6–10*). These data were further confirmed when we used different concentrations of EGF and HB-EGF for stimulation (supplemental Fig. S1).

To provide further evidence that HB-EGF-induced ubiquitylation of EGFR is, indeed, regulated by CD82, we used shRNA approach to selectively deplete CD82 in 2.5.2A breast cancer cells. Ubiquitylation of HB-EGF-stimulated EGFR in CD82-depleted cells increased (up to 3-fold) when compared with parental cells (Fig. 2*A*), confirming the role of CD82 in modulation of EGFR ubiquitylation. 2.5.2A cells express EGFR at a similar level to HB2 cells but have higher expression levels of CD82 (Fig. 1*A* and 2*B*).

Two ligands (HB-EGF and AR) that cause CD82-dependent decrease in ubiquitylation of EGFR contain heparin-binding domain, and we have previously reported that the activity of HB-EGF is controlled by its heparin-binding (HB) region via interaction with heparan sulfate proteoglycans (HSPG) (20). Thus, we examined whether HB domain of HB-EGF is essential for changes in the ubiquitylation of the receptor in cells expressing CD82. Notably, ubiqitylation of EGFR in both HB2

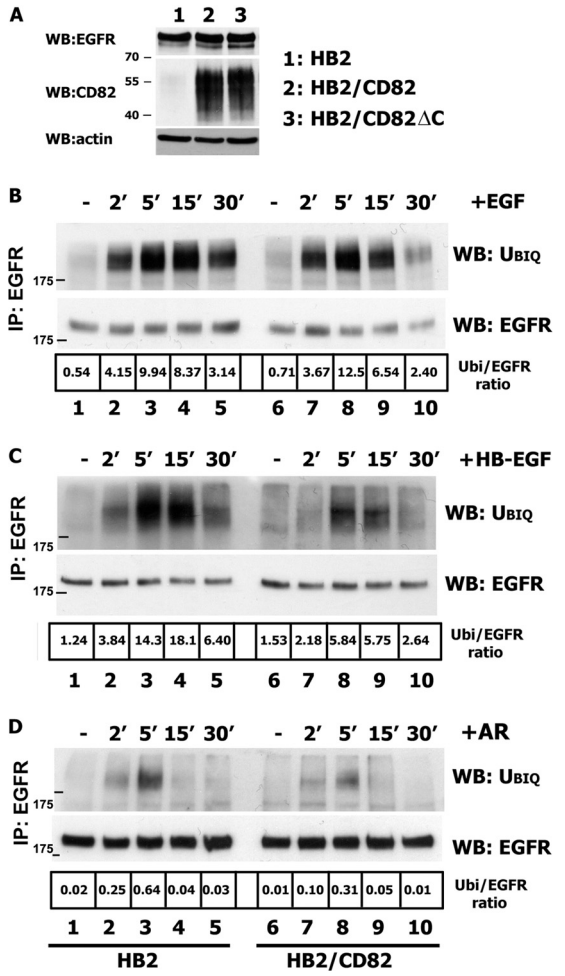

FIGURE 1. **Ubiquitylation of EGFR is impaired in CD82-overexpressing cells.** *A*, expression levels of CD82 and EGFR in HB2, HB2/CD82, and HB2/CD82ΔC cells were determined by Western blotting (*WB*) with anti-CD82 mAb (TS82b) or with anti-EGFR (Ab-15) mAb, respectively. WB with anti-actin mAb is a control for equal loading. *B–D*, HB2 and HB2/CD82 cells were serum-starved overnight and incubated with 15 ηg/ml EGF (*B*) or 20 ηg/ml HB-EGF (*C*) or 15 ηg/ml AR (*D*) for the indicated time intervals. After incubation, the cells were lysed in Triton X-100 (1%), EGFR was immunoprecipitated (*IP*) with anti-EGFR mAb (Ab-12; Neomarkers), and ubiquitylation (*UBIQ*) of the receptor was determined by Western blotting with anti-ubiquitin mAb (FK2; Enzo). The membranes were reblotted with anti-EGFR pAb (Cell Signaling). The results of one of three independent experiments are shown. Densitometric analysis was carried out on the films of equal exposure time using the ImageJ program.

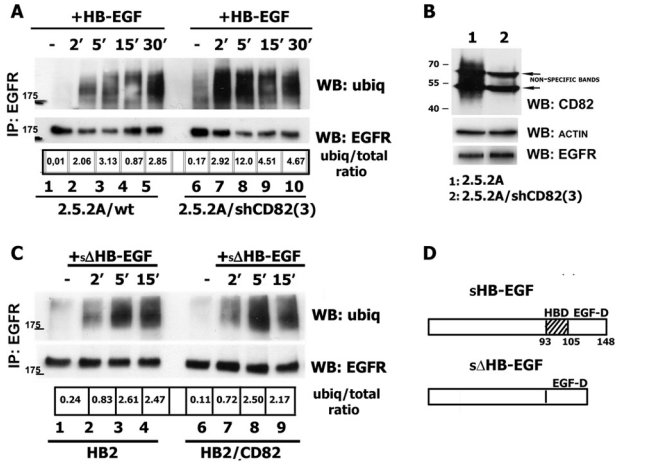

FIGURE 2. **Impairment of ubiquitylation of HB-EGF-stimulated EGFR is dependent on CD82 expression level and heparin-binding domain of the ligand.** *A*, 2.5.2A/wt and 2.5.2A/shCD82 cells were serum-starved overnight and incubated with 25 ηg/ml HB-EGF for indicated time intervals. After incubation, the cells were lysed in Triton X-100 (1%), EGFR was immunoprecipitated (*IP*) with anti-EGFR mAb (Ab-12; Neomarkers), and ubiquitylation (*ubiq*) of the receptor was determined by Western blotting (*WB*) with anti-ubiquitin mAb (FK2; Enzo). The membranes were reblotted with anti-EGFR pAb (Cell Signaling). The results of one of three independent experiments are shown. *B*, expression levels of CD82 and EGFR in 2.5.2A wild type and CD82 knockdown cells were determined by Western blotting with the appropriate antibodies. Equal loading was controlled by WB with anti-actin mAb. *C*, HB2, HB2/CD82 cells were serum-starved overnight, incubated with 10 ηg/ml sΔHB-EGF for indicated time intervals. Ubiquitylation of the receptor was determined by Western blotting with anti-ubiquitin mAb (FK2; Enzo) after immunoprecipitation as described above. The results of one of two independent experiments are shown. *D*, schematic structures of wild type and mutant forms of HB-EGF (adapted from Ref. 21).

and HB2/CD82 cell lines was robust and comparable following stimulation with sΔHB-EGF, HB-EGF with deleted HB domain (Fig. 2, *C* and *D*). The changes in ubiquitylation after stimulation with sΔHB-EGF could not be attributed to the different receptor-binding parameters of the ligand because we have reported earlier that binding of soluble ΔHB-EGF is comparable with that of the wild type (21). The lower total ubiquitylation levels in these experiments were due to the lower concentration of the ligand (10 ηg/ml). Taken together, these data indicate that CD82 selectively regulates ligand-induced ubiquitylation of EGFR through a novel mechanism that possibly involves surface heparan sulfate proteoglycans.

Postendocytic Trafficking of CD82 and Activated EGFR—We expected that CD82-dependent decrease in EGFR ubiquitylation would affect intracellular trafficking of the receptor. Thus, we investigated trafficking of the receptor in HB-EGF-stimulated cells in more detail. It is well established that activated EGFR is initially delivered to the EEA1-positive endosomes (26). Hence, we compared the dynamics of EGFR trafficking through this compartment in HB2 and HB2/CD82 cells after stimulation with HB-EGF. The cells were incubated with ligand on ice for 1 h, then washed, and transferred to 37 °C for indicated time intervals. Then cells were fixed, permeabilized, and labeled for EGFR and EEA1 (Fig. 3*A*). Quantification analysis of the collected z-stacks of images showed that after 2 min of incubation with HB-EGF, the proportion of EGFR co-localized with EEA1 was significantly higher in control cells (Fig. 3*B*) (27% in HB2 and 17% in HB2/CD82 cells). The difference was also observed in cells after 5 min of incubation, although less pronounced (Fig. 3*B*) (37% for HB2/CD82 cells and 30% for the control cells). Maximum (and comparable) co-localization has been reached after 15 min in both cell lines (38 and 43%, respectively) with sharp decline (from 43% to 30%) in HB2/CD82 cells at 30 min (Fig. 3*B*). In contrast, in HB2 cells co-localization of EGFR with EEA1 did not change over the 5–30-min time interval. We conclude that we observed slow delivery of EGFR to EEA1-positive endosomes and fast egress from this compartment in HB2/CD82 cells. In contrast, EGFR in control cells was fast delivered to and retained in EEA1-labeled endosome over the indicated time interval.

We also investigated intracellular trafficking of EGFR in cells expressing CD82ΔC (C-terminal deletion mutant of CD82). Interestingly, recruitment of EGFR to the EEA1-positive compartment at earlier time points in these cells was comparable

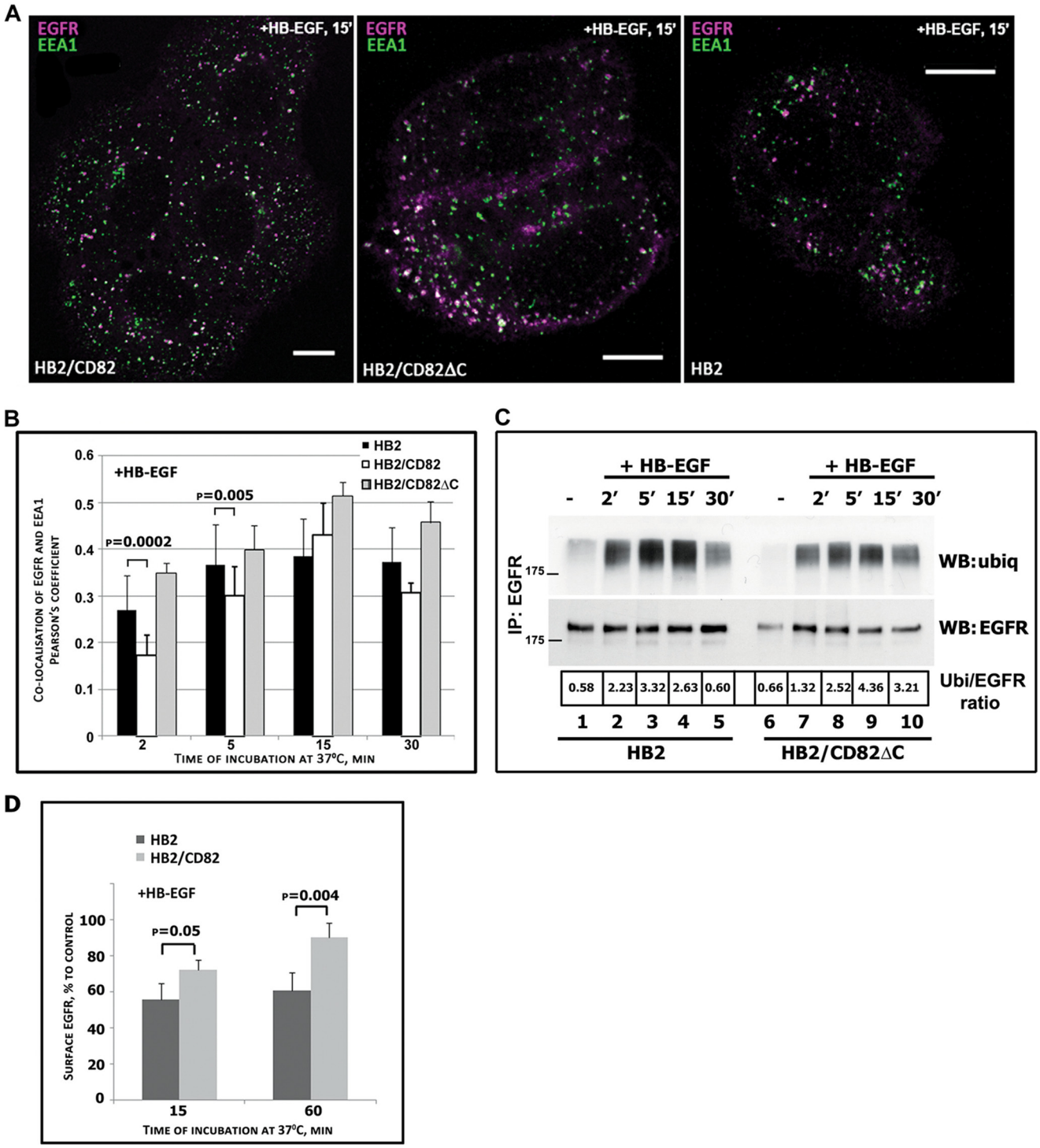

FIGURE 3. **Postendocytic trafficking of EGFR following HB-EGF stimulation is altered in the presence of CD82.** *A* and *B*, HB2, HB2/CD82wt, and HB2/CD82ΔC cells plated on coverslips were serum-starved overnight and incubated with HB-EGF (25 ηg/ml) at 37 °C for indicated time intervals. The cells were fixed and labeled for EGFR (anti-EGFR mAb; Ab-15) and the early endosomal marker EEA1 (anti-EEA1 mAb; Transduction Labs) (as described under "Experimental Procedures"). *A*, Representative confocal images of the cells following 15 min of EGFR internalization. *Bars*, 10 μm. *B*, quantification of the amount of EGFR co-localizing with EEA1 in an average of 40–50 cells for each time point is presented as Pearson's coefficient (average of three experiments). The *p* values were determined by paired two-tailed *t* test. *C*, ubiquitylation (*ubiq* or *Ubi*) of EGFR in HB2 and HB2/CD82ΔC cells was determined by immunoprecipitation (*IP*) as described under "Experimental Procedures." The results of one of three independent experiments are shown. *D*, time course of EGFR recycling in HB2 and HB2/CD82 cells following stimulation with HB-EGF. The cells were incubated on ice with the ligand, washed, and incubated at 37 °C for indicated time intervals. The amount of EGFR at the cell surface was determined by flow cytometry. The values presented are means (percentages) ± S.D. from four experiments. *WB*, Western blotting.

with that seen in control cells (Fig. 3*B*). Thus, deletion of the C-terminal part of CD82 renders this protein inactive toward EGFR in this assay. Because we proposed that CD82-dependent differences in HB-EGF-induced trafficking may be due to decreased ubiquitylation of EGFR, it was important to compare ubiquitylation kinetics in the control and CD82ΔC-expressing

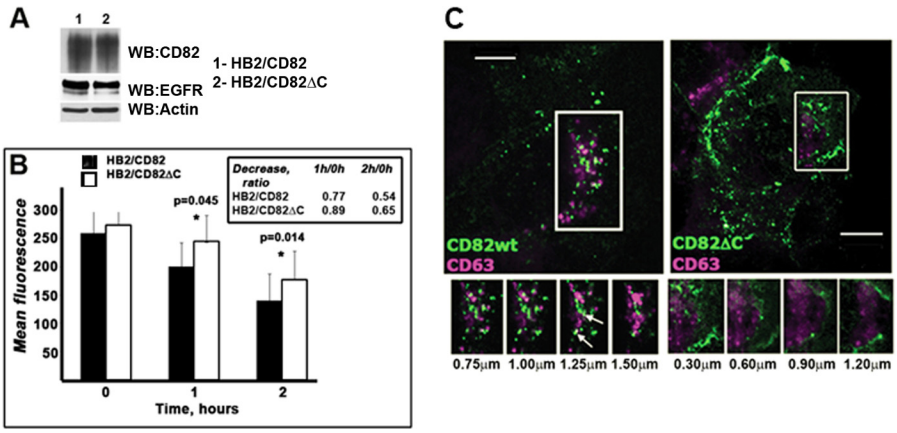

FIGURE 4. **Mutation in C-terminal of CD82 changes intracellular trafficking of the tetraspanin.** *A*, expression levels of CD82wt and CD82ΔC determined by Western blotting (*WB*). *B*, internalization rate of CD82 in HB2/CD82 and HB2/CD82ΔC cells was studied using microplate internalization assay as described under "Experimental Procedures." Internalization of anti-CD82 mAb (IA4 or TS82b) was monitored (after 1 and 2 h of chase at 37 °C) with IRDye 800CW and Odyssey Infrared Imaging System (LI-COR Biosciences). The graph presents average of mean fluorescence values from three experiments (± S.D.) for each cell line at indicated time point. The values presented in the table are ratios at particular time points relative to values at zero time point. The *p* value for each time point was determined in paired two-tailed *t* test. *C*, representative confocal images following uptake of anti-CD82 mAb (IA4) after 1 h of chase in cells expressing CD82wt or CD82ΔC are shown. The cells were acid-washed, fixed, permeabilized, and co-stained with anti-CD63 (1B5) mAb (as described under "Experimental Procedures"). Co-localization of CD82 and CD63 was assessed using isotype specific Alexa Fluor-conjugated goat anti-mouse antibodies. Z-sections were taken at the interval of 0.30–0.35 μm. *Scale bar*, 10 μm.

cells. As illustrated in Fig. 3*C*, HB-EGF-induced ubiquitylation of EGFR in HB2/CD82ΔC cells was even increased when compared with HB2 cells. Taken together, these data show that CD82-dependent attenuation of EGFR ubiquitylation in cells stimulated with HB-EGF correlates with the delayed recruitment of the receptor to EEA1-positive endosomes and accelerated egress from these compartments. Importantly, this activity of CD82 is dependent on the cytoplasmic C-terminal part of the protein.

Decreased ubiquitylation and changed dynamics of recruitment to early endosomes may be an indication of the receptor's diversion to a recycling route. We compared cell surface levels of EGFR after HB-EGF stimulation in HB2 control and HB2/CD82 cells as measured in pulse-chase experiments by flow cytometry (Fig. 3*D*). In accordance with the ubiqitylation data described above, the number of HB-EGF-activated receptors on the cell surface in HB2/CD82 cells was higher than in control cells (15 min after stimulation). Furthermore, after 60 min incubation with HB-EGF the number of receptors was increased. Although the newly synthesized receptors were not taken into account in these experiments, the number would not be greatly changed because of a relatively short time course. Taken together, these data clearly indicate that CD82 expression alters trafficking routes of HB-EGF-stimulated EGFR.

Trafficking of CD82 Is Controlled by the C-terminal Cytoplasmic Domain of the Protein—The C-terminal cytoplasmic region deleted in CD82ΔC mutant contains a classical tyrosine-based sorting signal (YSKV). As we have described above, its deletion negated effects of CD82 on the ubiquitylation and intracellular trafficking of EGFR.

Thus, it was important to compare trafficking routes of CD82wt and CD82ΔC from the plasma membrane in more detail. Initially, we measured the rate of the mAb-induced internalization of CD82 using a microplate internalization assay in cells stably transfected with CD82wt or CD82ΔC (the expression levels of both proteins were comparable; Fig. 4*A*). The internalization rate of antibody-bound CD82wt was slow with only ~23% of CD82wt being removed from the cell surface after 1 h of chase (Fig. 4*B*). After 2 h of chase ~54% of CD82wt could still be detected at the cell surface. Internalization of antibody-bound CD82ΔC appeared to be even slower with only ~11% of the protein being removed after 1 h and ~35% being removed after 2 h (Fig. 4*B*). Immunofluorescence analysis of the internalized CD82 at the 1-h time point following anti-CD82 mAb binding illustrated the difference in the distribution patterns of CD82wt and CD82ΔC (Fig. 4*C*). The wild type protein was found in round puncta in perinuclear area (Fig. 4*C*, *left panel*). On the other hand, internalized CD82ΔC was found in the CD63-negative "polymorphic" structures close to the plasma membrane (Fig. 4*C*, *right panel*).

We also studied the distribution of internalized CD82wt and CD82ΔC between various intracellular compartments by electron microscopy. We used two different approaches: immunogold labeling of cryosections prepared from the cells after antibody chase and EPON embedding of the samples after chase with antibody-bound gold. The images from the second set of experiments are shown because they are more illustrative. After 5 min of chase at 37 °C, gold-labeled CD82 was found at the plasma membrane (Fig. 5*A*, *arrows*) and in the uncoated invaginations of plasma membrane (PM) (Fig. 5*B*, *arrows*). Interestingly, CD82 was not detected in coated invaginations of the PM (Fig. 5*C*, *arrowheads*), but it was found on the uncoated internal vesicles (Fig. 5*C*, *arrows*). CD82 could often be detected in the rosette-like endosomal structures, thereby highlighting the diversity of CD82 trafficking pathways (Fig. 5, *D*, *arrows*, and *K*). After a 60-min chase, CD82 was distributed in various multivesicular endosomes at different stages of biogenesis and at the PM (Fig. 5, *E* and *F*, *arrows*). Occasionally, gold-labeled CD82 was found on extracellular vesicles (Fig. 5*F*). Lack of a visible coat and the morphology of the PM invaginations labeled for CD82, together with the data from siRNA knockdown experi-

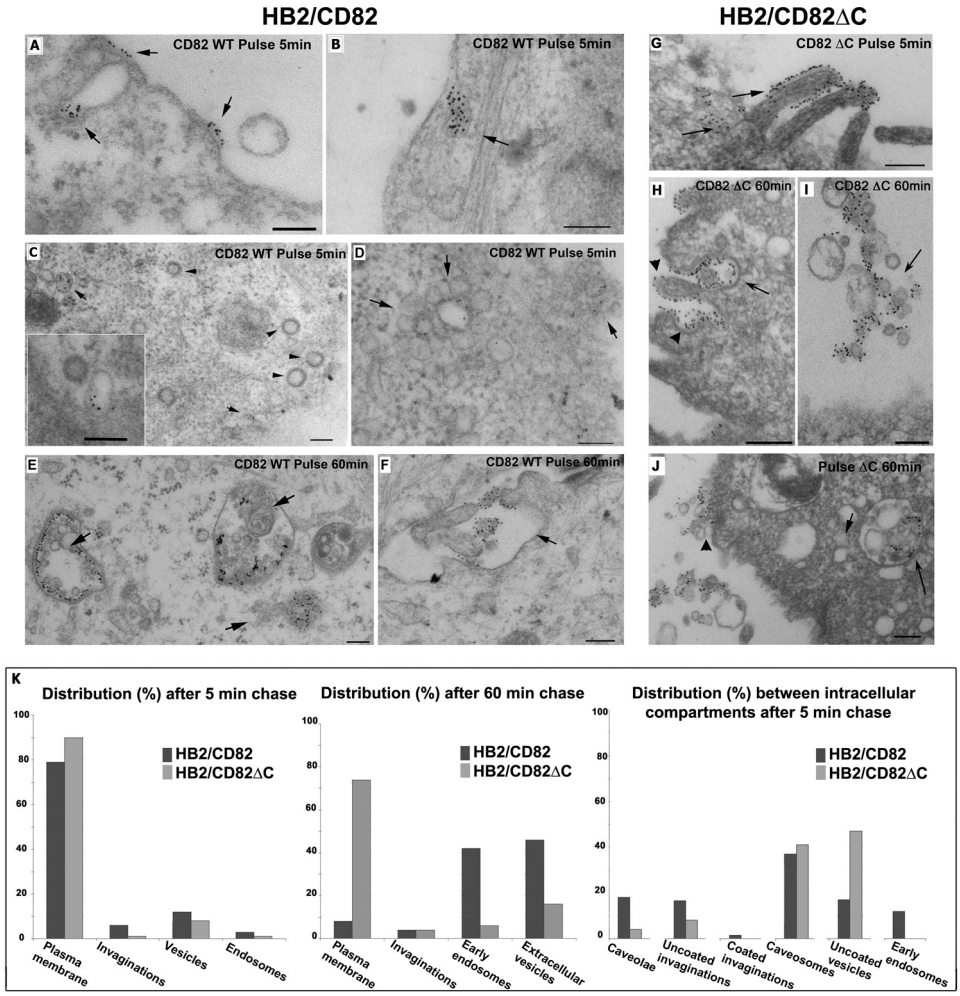

FIGURE 5. **Distribution of CD82 after 5 and 60 min of chase with anti-CD82 mAb analyzed by electron microscopy.** HB2/CD82wt and HB2/CD82ΔC were incubated with anti-CD82 mAb (TS82b) for 1 h and then with protein A gold 10 nm for 40 min at 4 °C and subsequently chased for 5 or 60 min at 37 °C. Then the cells were fixed and processed according to the protocol described under "Experimental Procedures." *A*, *B*, and *G*, after 5 min of chase, CD82wt and CD82ΔC were distributed to the plasma membrane and in the uncoated invaginations of PM. *C* (*main panel* and *inset*), after 5 min of chase, internalized CD82wt was found in the uncoated structures (*arrow*) but not coated vesicles (*arrowheads*). *D*, after 5 min of chase, CD82wt was observed in rosette-like endosomal structures. *E*, after 60 min of chase, internalized CD82wt was mainly distributed to the intracellular multivesicular compartments (*arrows*) and found occasionally at the PM. *F*, after 60 min of chase, gold-labeled CD82wt was also found on extracellular vesicles (*arrows*). *H–J*, CD82ΔC after 60 min chase was found on internal (*H* and *J*) and on extracellular (*I*) vesicles. *K*, quantification of the distribution of gold particles (average 1500) between various membranous compartments after 5 and 60 min of chase with anti-CD82 mAb in HB2/CD82wt and HB2/CD82ΔC cells. *Scale bar*, 200 nm.

ments of AP-2 (data not shown), excluded involvement of clathrin-coated pits in the internalization of CD82.

Similarly to the wild type, after a 5-min chase, the C terminus deletion mutant of CD82 (CD82ΔC) was found mainly at the cell surface and in the uncoated invaginations (Fig. 5*G*, *arrows*). At a later time point (60 min), CD82ΔC was occasionally found in multivesicular endosomes/lysosomal structures with enlarged internal vesicles (Fig. 5, *H* and *J*, *arrows*) and on the extracellular vesicles (Fig. 5*I*, *arrow*), but it was mainly distributed at the PM (Fig. 5, *H* and *J*, *arrowheads*). Study of the intracellular morphology and quantification of immunogold labeling data confirmed that the C-terminal cytoplasmic domain is involved in the postendocytic sorting and intracellular trafficking of CD82 (Fig. 5*K*). Compartmental distribution of CD82 and CD82ΔC after internalization was profoundly different (Fig. 5, *A–K*).

Having established the importance of the C-terminal cytoplasmic region in trafficking of CD82, we next examined the co-trafficking of EGFR and CD82 after stimulation with HB-EGF. To follow trafficking of the receptor in relation to the surface pool of CD82, these experiments were performed in the presence of anti-CD82 mAb (we found that the presence of this antibody did not affect ligand binding to EGFR or did not alter receptor-mediated signaling (not shown)). Cells were incubated with the ligand and antibody on ice for 1 h, then washed, and incubated at 37 °C for various time intervals. We observed partial co-localization of internalized EGFR and CD82 proteins at all time points: the receptor and tetraspanin were detected in vesicles localized in close proximity to the plasma membrane and in the perinuclear region (Fig. 6*A*). The quantification analysis of confocal images demonstrated a substantial degree of co-localization of the internalized receptor and the wild type CD82 throughout the 60-min chase: the difference in co-localization between the first and last time points was ~13% (Fig. 6*B*). Notably, the co-localization for the EGFR-CD82ΔC pair in a similar assay

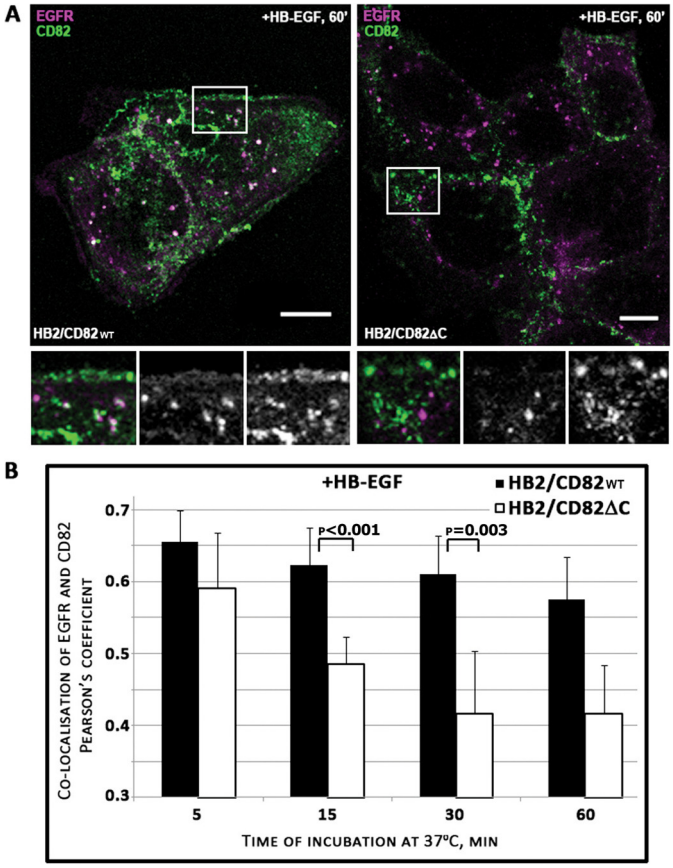

FIGURE 6. **Co-localization of internalized CD82 and EGFR after HB-EGF stimulation.** HB2/CD82 and HB2/CD82ΔC cells were incubated with HB-EGF (25 ηg/ml) and anti-CD82 mAb (TS82b) at 4 °C for 1 h. After three washes, the cells were chased at 37 °C for the indicated time intervals. The cells were fixed, permeabilized, and co-stained with anti-EGFR mAb. Co-localization of CD82 and EGFR was assessed using isotype specific Alexa Fluor-conjugated goat anti-mouse antibodies. *A*, representative confocal images of cells following 60 min of chase are presented. *Scale bar*, 10 μm. *B*, quantification of co-localized EGFR and CD82 after internalization was calculated in an average 40–50 cells at each time point in each cell line after collection of z-sections. The data are presented as Pearson's coefficient. The values are means from three independent experiments. The *p* values were determined by paired two-tailed *t* test.

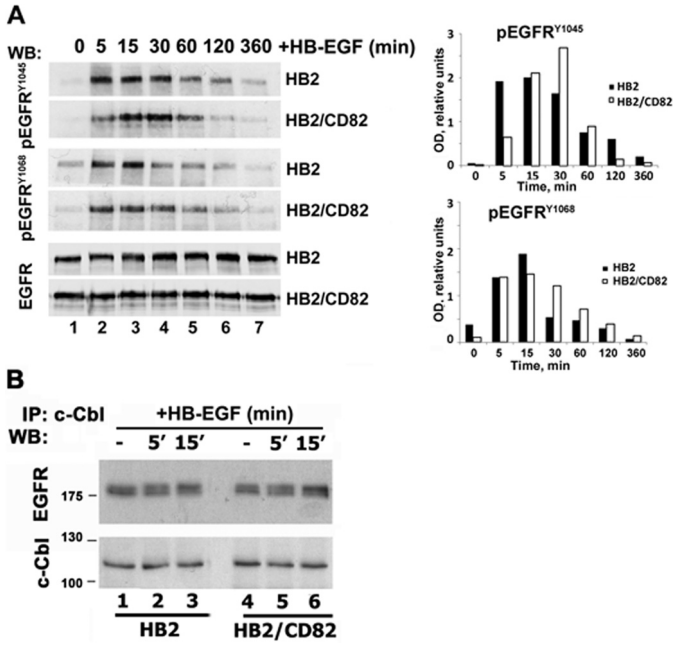

FIGURE 7. **CD82 and recruitment of c-Cbl to HB-EGF-stimulated EGFR.** *A*, serum-starved HB2 and HB2/CD82 cells were incubated with HB-EGF (15 ηg/ml) at 37 °C for indicated time intervals. Equal amounts of protein (~10 μg) were loaded onto polyacrylamide gels, and kinetics of phosphorylation was determined by Western blotting (*WB*) with the appropriate antibodies. Blots were developed using HRPO-conjugated secondary antibody from Dako. The levels of total EGFR were also tested. The data presented are from one of three independent experiments. Quantification of this experiment is shown in a graph. Densitometry was carried out using ImageJ. *B*, interaction of c-Cbl with EGFR in HB-EGF-stimulated cells was studied by immunoprecipitation (*IP*) with anti-c-Cbl antibody. EGFR was detected by Western blotting with anti-EGFR polyclonal antibody as described under "Experimental Procedures." The same membrane was redeveloped with anti-c-Cbl goat antibody. The results of a representative experiment are shown (three in total).

was considerably decreased with the corresponding difference being more than 33%. These data indicate that the C-terminal region is important for a prolonged association of CD82 with EGFR in endocytic compartments, and the divergence in trafficking routes between the wild type protein and the mutant may, indeed, underlie the functional deficiency of the CD82ΔC toward EGFR after HB-EGF stimulation.

CD82 Regulates Serine Phosphorylation of c-Cbl in HB-EGF-stimulated Cells: the Role of PKC—Ligand-induced ubiquitylation of EGFR is dependent on the interaction of Cbl E3 ubiquitin ligases with the activated receptor (17). Phosphorylation of the receptor on Tyr^{1045} and Tyr^{1068} leads to the direct or indirect (via Grb2) recruitment of c-Cbl (28). First, we studied HB-EGF induced phosphorylation of EGFR on Tyr^{1045} and Tyr^{1068} in both HB2/CD82 and control cells (Fig. 7*A*). Although there were minor variations in phosphorylation at individual time points, we observed no consistent differences in kinetics of Tyr^{1068} phosphorylation between the cell lines. On the other hand, presence of CD82 affected the kinetics of Tyr^{1045} phosphorylation. In the control cells, phosphorylation of Tyr^{1045} peaked at 5–15 min (Fig. 7*A*, *top panel*). This correlated with the kinetics of ubiquitylation of HB-EGF-activated receptor in HB2 cells (see above). In contrast, phosphorylation of the receptor on this residue in HB2/CD82 cells was minimal at the 5-min time point and then steadily increased up to 30 min (Fig. 7*A*). Notably, phosphorylation of Tyr^{1045} at the 5-min time point in HB2/CD82 cells was ~2.5 times lower when compared with control cells (Fig. 7*A*, compare *lane 2*, *two top panels*). We also observed that decay of Tyr^{1045} phosphorylation was faster in CD82-expressing cells over extended time course (Fig. 7*A*, *lanes 6* and *7*, *two top panels*). Notably, despite these differences, the interaction between EGFR and c-Cbl was not affected by either the presence of CD82 or the treatment of cells with HB-EGF (Fig. 7*B*). Therefore, we concluded that CD82 dependent differences in ubiquitylation are not due to differential assembly of the EGFR-Cbl complex in the control and HB2/CD82 cells.

The activity of c-Cbl is regulated by tyrosine and serine phosphorylation of the protein (29, 30). Thus, we investigated whether phosphorylation of c-Cbl upon HB-EGF stimulation is affected in the presence of CD82. Although we observed no qualitative or quantitative differences in phosphorylation of c-Cbl on tyrosines 774 and 731 in HB2 and HB2/CD82 cells

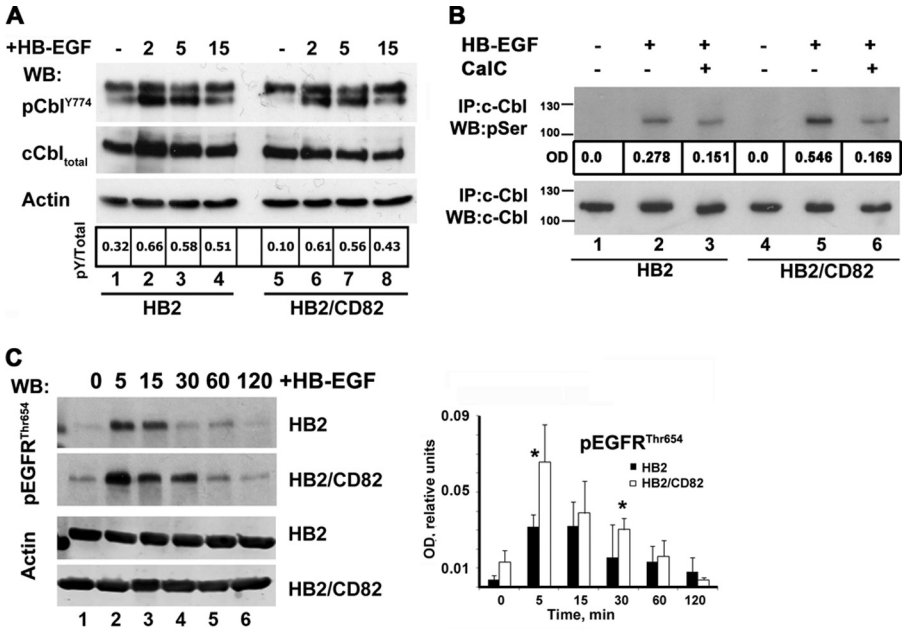

FIGURE 8. **CD82 modulates PKC-dependent phosphorylation of EGFR and c-Cbl in HB-EGF-stimulated cells.** *A*, phosphorylation of c-Cbl on Tyr^{774} was studied by Western blotting (*WB*) with phosphospecific anti-Cbl antibody in cells (HB2 and HB2/CD82) stimulated with HB-EGF. Total c-Cbl and actin were used as control for loading. *B*, serine phosphorylation of c-Cbl in HB-EGF-stimulated cells (HB2 and HB2/CD82) was studied by immunoprecipitation (*IP*) with anti-c-Cbl mAb followed by Western blotting with anti-phosphoserine polyclonal antibody. The same membrane was redeveloped with anti-c-Cbl polyclonal antibody to confirm that equal amount of protein was immunoprecipitated in each sample. In parallel experiments, cells were pretreated for 1.5 h with 5 μM (final concentration) of anti-PKC inhibitor Calphostin C (*CalC*) before stimulation with HB-EGF. The data presented are from one of three independent experiments. *C*, phosphorylation of EGFR on Thr^{654} was studied by Western blotting with phosphospecific anti-EGFR^{Thr654} antibody (Millipore). The blot is a representative of three independent experiments. Quantification of three experiments is presented on the graph. The *p* value was determined in paired two-tailed *t* test.

(Fig. 8*A*, and data not shown), HB-EGF-induced serine phosphorylation of c-Cbl was more pronounced (by ~2-fold) in CD82-expressing cells (Fig. 8*B*, *lanes 2* and *5*). PKCα has been reported to phosphorylate c-Cbl on serine residues (30, 31). Given that CD82 is known to recruit PKC to plasma membrane (32), we investigated to what degree PKC is responsible for serine phosphorylation of c-Cbl in HB-EGF-stimulated cells. We used the specific inhibitor of PKC Calphostin C for treating control and CD82-expressing cells before and during stimulation with HB-EGF. Serine phosphorylation of c-Cbl was decreased by almost 3-fold in HB2/CD82 cells compared with 1.5-fold in control cells (Fig. 8*B*, *lanes 3* and *6*). We concluded that PKC contributes to serine phosphorylation of c-Cbl following HB-EGF phosphorylation, and this is more pronounced in the presence of CD82.

To explore the connection between CD82, PKC and ubiquitylation of EGFR further, we analyzed phosphorylation of the receptor on Thr^{654}. PKC-dependent phosphorylation of this residue in the juxtamembrane domain of EGFR has been previously linked with suppression of EGFR ubiquitylation and diversion of receptor trafficking toward recycling (33, 34). We found that phosphorylation of EGFR on Thr^{654} was significantly increased in CD82-expressing cells after stimulation with HB-EGF (more than 2-fold at the 5-min time point) (Fig. 8*C*, *lane 2*, *top two panels*). Furthermore, Thr^{654} phosphorylation lasted longer in HB2/CD82 cells when compared with the control cells (Fig. 8*C*, *lanes 4–6*). Taken together, these data indicate that CD82 can regulate HB-EGF-induced ubiquitylation of EGFR at multiple levels through mechanisms involving PKC.

DISCUSSION

The role of tetraspanin proteins in regulation of various signal transduction pathways has been well documented (3). It has been proposed that tetraspanins function via specialized membrane microdomains by modulating activities of the associated signaling receptors (*e.g.*, integrins, ErbB proteins). Here we describe a novel pathway that implicates tetraspanins in regulation of ubiquitylation of their molecular partners. Specifically, we demonstrate that the metastasis suppressor tetraspanin KAI-1/CD82 controls ligand-induced ubiquitylation of EGFR.

Perhaps one of our most intriguing discoveries is a specific effect of CD82 on ubiquitylation and trafficking of EGFR activated by growth factors with heparin-binding domains (HB-EGF and AR). Variations in ubiquitylation of EGFR were attributed to differences in affinities of specific ligand-receptor pairs (26, 27). Our results show for the first time that ligand-dependent differential ubiquitylation of EGFR is also controlled by CD82, a tetraspanin protein, which we previously described as a molecular partner for the receptor (5). Furthermore, CD82-dependent molecular mechanisms (discussed below) are unlikely to rely on either differential ligand affinities or pH sensitivities of HB-EGF/AR-EGFR complexes. Indeed, we found that HB-EGF-induced phosphorylation of the receptor's autophosphorylation site Tyr^{1068} at the early time points was comparable in both cell lines, thereby excluding the differences in ligand binding.

It has been previously reported that different ligands dictate the postendocytic itinerary of activated EGF receptor (26), and this correlates with the extent of EGFR ubiquitylation upon

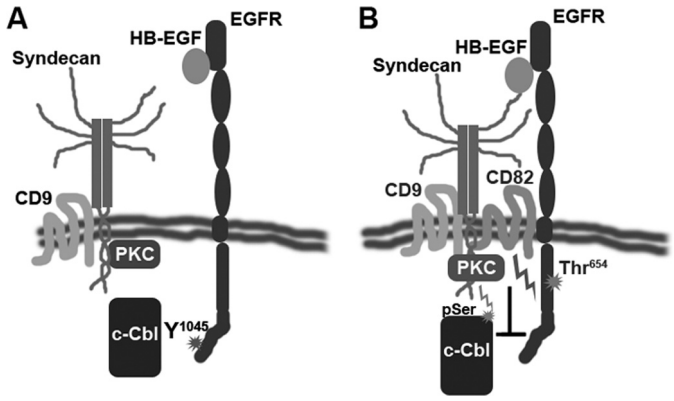

FIGURE 9. **CD82 links HSPG-activated PKC, ligand-bound EGFR and c-Cbl.** The model depicts the role of CD82 in early events of EGFR activation by heparin-binding domain containing ligand (*e.g.*, HB-EGF). *A*, in absence of CD82 EGFR is not recruited to the tetraspanin-enriched microdomains. HB-EGF binding leads to robust phosphorylation of the receptor, recruitment of c-Cbl, and further ubiquitylation. *B*, when CD82 is expressed, a subset of EGFR associated with the tetraspanin is recruited to TERM where it is placed in close proximity to syndecans. Stimulation with HB-EGF leads to activation of PKC recruited to TERM by syndecans and CD82. PKC attenuates EGFR signaling by affecting c-Cbl recruitment to this subset of receptors. Additionally, active PKC negatively regulates activity of E3 ligase by serine/threonine phosphorylation.

ligand binding. Although more pronounced ubiquitylation is typically linked to increased targeting of the receptor to lysosomes (26), it has been also reported that the level of ubiquitylation does not always correlate with degradation of EGFR (35). Indeed, our results show that despite differences in EGFR ubiquitylation, total levels of the receptor in HB2 and HB2/CD82 cells remain similar and unchanged over the extended period of exposure to HB-EGF (Fig. 7*A*). Thus, our data indicate that CD82-dependent differences in HB-EGF-induced ubiquitylation most likely affect trafficking pathways preceding lysosomal targeting of EGFR.

What could be the mechanisms underlying the regulatory specificity of CD82 toward ligand-induced ubiquitylation of EGFR? Our data with sΔHB variant of HB-EGF strongly suggest that CD82 acts via HSPG. Binding of many heparin-binding growth factors including HB-EGF and AR to their receptors is influenced by HSPG (21, 36, 37). These ligand-HSPG interactions may either enhance or attenuate the activity of the receptors (20, 21). Importantly, it has previously been reported that the activity of HB-EGF (but not EGF) is dependent on syndecans, the most prominent family of cell-associated proteoglycans (38, 39). Therefore, one can envisage a scenario whereby CD82 and its tetraspanin partners (*e.g.*, CD9, which is known to associate with syndecans (3, 5)) facilitate formation of the tripartite EGFR-growth factor-HSPG complex, which activates not only receptor but also HSPG. CD82 and activated HSPG (*e.g.*, syndecans) could, in turn, recruit PKCα (40, 41), thereby increasing effective concentration of the enzyme in proximity to its targets (*i.e.*, EGFR, c-Cbl). Consequently, increased phosphorylation of threonine 654 in EGFR on one hand and serine phosphorylation of c-Cbl on the other would lead to changes in both ligand-induced ubiquitylation of the receptor and alteration of its postendocytic trafficking route (33) (Fig. 9). Although the proposed model explains the regulatory specificity of CD82 toward various EGFR ligands (indeed, the activity of CD82 can be observed only when growth factors engage HSPG), future work will be required to establish molecular mechanisms underlying the CD82-dependent functional dynamics between the complexes of HSPG-PKC on one side and EGFR-c-Cbl on the other.

We found that reduction of HB-EGF-induced ubiquitylation of EGFR also influenced its intracellular trafficking: dynamics of receptors' recruitment to the early/sorting endosomes and their egress from these compartments were changed in CD82-expressing cells. The timing of EGFR co-localization with EEA1-containing endosomes was delayed, which could be due to the altered ubiquitylation and subsequent endocytosis of the receptors associated with HSPG in TERM. Syndecans are known to mediate endocytosis of heparin-binding ligands and proteins (*e.g.*, FGF2 or eosinophil cationic protein) by macropinocytosis (42, 43). This pathway is slow and involves formation of uncoated vesicles that eventually fuse with sorting endosomes. The fate of the cargo-HSPG complex is decided according to the ubiquitylation status of cargo or HSPG (*e.g.*, syndecans) interactions (44, 45) and may progress either to the lysosomal degradation or to the recycling route (44). The role of CD82 in this diversion could be in bringing EGFR in proximity to HSPG and regulating ubiquitylation on one side (discussed above) and in providing suitable lipid surroundings (*e.g.*, gangliosides and/or cholesterol content) on the other (6).

Our report demonstrates for the first time the functional importance of the C-terminal cytoplasmic part of CD82: deletion of this region compromises the activity of this tetraspanin toward EGFR upon stimulation with HB-EGF. Importantly, functional deficiency of CD82ΔC correlates with changes in the endocytic trafficking of this mutant. First, we found that the C-terminal cytoplasmic region regulates internalization of CD82. Given that this part of the protein carries a "classical" tyrosine-based motif (YSKV), the involvement of AP-2 and, consequently, clathrin would be anticipated. However, our electron microscopy data clearly demonstrate that CD82 is excluded from the clathrin-coated pits and coated vesicles. These results further strengthen a recent observation by Xu *et al.* (15), who showed that CD82 is internalized via clathrin- and dynamin-independent pathway(s). Second, we found that endocytosed CD82ΔC mutant (but not the wild type protein) is concentrated in the polymorphic compartment close to the plasma membrane. Although the exact identity of these structures remains unknown, these results strongly suggest that the C-terminal region of CD82 also contributes to postendocytic trafficking of the protein. How does the deficiency in trafficking affect the activity of CD82ΔC toward EGFR? We observed that the time of co-localization with the HB-EGF-activated receptor is decreased for the mutant when compared with the wild type CD82. Hence, a possible physical link between HB-EGF-bound EGFR and HSPG (see above) may also be short-lived (or destabilized) in CD82ΔC-expressing cells.

In summary, our results describe CD82 as a novel regulator of ligand-induced ubiquitylation of EGF receptor. This newly established activity of CD82 suggests a new paradigm in tetraspanin-dependent regulation of endocytic trafficking of the associated transmembrane cargos. Although HB-EGF is a potent mitogen for various cell types, its binding may also lead

to decreased proliferation in certain cellular contexts (20). Although the underlying mechanisms of the HB-EGF opposing activities are still unknown, it is not unfeasible that the differential expression of CD82 and its involvement in ligand-induced ubiquitylation of EGFR is, in fact, a critical factor that controls the alternative signaling pathways.

Acknowledgments—We are grateful to all our colleagues for providing antibodies and reagents. We thank Drs. Cindy Miranti and Eric Rubinstein for valuable discussions and advice. We thank Alexandra Berditchevskaia for editorial help.

REFERENCES

1. Berditchevski, F. (2001) Complexes of tetraspanins with integrins. More than meets the eye. *J. Cell Sci.* **114,** 4143–4151
2. Hemler, M. (2003) Tetraspanin proteins mediate cellular penetration, invasion, and fusion events and define a novel type of membrane microdomain. *Annu. Rev. Cell Dev. Biol.* **19,** 397–422
3. Charrin, S., le Naour, F., Silvie, O., Milhiet, P.-E., Boucheix, C., and Rubinstein, E. (2009) Lateral organisation of membrane proteins. tetraspanins spin their web. *Biochem. J.* **420,** 133–154
4. Berditchevski, F., and Odintsova, E. (2007) Tetraspanins as regulators of protein trafficking. *Traffic* **8,** 89–96
5. Odintsova, E., Sugiura, T., and Berditchevski, F. (2000) Attenuation of EGF receptor signaling by a metastasis suppressor, the tetraspanin CD82/KAI-1. *Curr. Biol.* **10,** 1009–1012
6. Odintsova, E., Butters, T. D., Monti, E., Sprong, H., van Meer, G., and Berditchevski, F. (2006) Gangliosides play an important role in the organization of CD82-enriched microdomains. *Biochem. J.* **400,** 315–325
7. He, B., Liu, L., Cook, G. A., Grgurevich, S., Jennings, L. K., and Zhang, X. A. (2005) Tetraspanin CD82 attenuates cellular morphogenesis through down-regulating integrin alpha6-mediated cell adhesion. *J. Biol. Chem.* **280,** 3346–3354
8. Sridhar, S. C., and Miranti, C. K. (2006) Tetraspanin KAI1/CD82 suppresses invasion by inhibiting integrin-dependent crosstalk with c-Met receptor and Src kinases. *Oncogene* **25,** 2367–2378
9. Takahashi, M., Sugiura, T., Abe, M., Ishii, K., and Shirasuna, K. (2007) Regulation of c-Met signaling by the tetraspanin KAI-1/CD82 affects cancer cell migration. *Int. J. Cancer* **121,** 1919–1929
10. Miranti, C. K. (2009) Controlling cell surface dynamics and signalling. How CD82 suppresses metastasis. *Cell. Signal.* **21,** 196–211
11. Tsai, Y. C., and Weissman, A. M. (2011) Dissecting the diverse functions of the metastasis suppressor CD82/KAI1. *FEBS Lett.* **585,** 3166–3173
12. Danglot, L., Chaineau, M., Dahan, M., Gendron, M. C., Boggetto, N., Perez, F., and Galli, T. (2010) Role of TI-VAMP and CD82 in EGFR cell-surface dynamics and signaling. *J. Cell Sci.* **123,** 723–735
13. Escola, J. M., Kleijmeer, M. J., Stoorvogel, W., Griffith, J. M., Yoshie, O., and Geuze, H. J. (1998) Selective enrichment of tetraspan proteins on the internal vesicles of multivesicular endosomes and on exosomes secreted by human B-lymphocytes. *J. Biol. Chem.* **273,** 20121–20127
14. Vyas, J. M., Kim, Y.-M., Artavanis-Tsakonas, K., Love, J. C., Van der Veen, A. G., and Ploegh, H. L. (2007) Tubulation of class II MHC compartments is microtubule dependent and involves multiple endolysosomal membrane proteins in primary dendritic cells. *J. Immunol.* **178,** 7199–7210
15. Xu, C., Zhang, Y. H., Thangavel, M., Richardson, M. M., Liu, L., Zhou, B., Zheng, Y., Ostrom, R. S., and Zhang, X. A. (2009) CD82 endocytosis and cholesterol-dependent reorganization of tetraspanin webs and lipid rafts. *FASEB J.* **23,** 3237–3288
16. Sigismund, S., Confalonieri, S., Ciliberto, A., Polo, S., Scita, G., and Di Fiore, P. P. (2012) Endocytosis and signaling. Cell logistics shape the eukaryotic cell plan. *Physiol. Rev.* **92,** 273–366
17. Sorkin, A., and Goh, L. K. (2009) Endocytosis and intracellular trafficking of ErbBs. *Exp. Cell Res.* **315,** 683–696
18. Shearer, M., Bartkova, J., Bartek, J., Berdichevsky, F., Barnes, D., Millis, R., and Taylor-Papadimitriou, J. (1992) Studies of clonal cell lines developed from primary breast cancers indicate that the ability to undergo morphogenesis in vitro is lost early in malignancy. *Int. J. Cancer* **51,** 602–612
19. Berditchevski, F., Odintsova, E., Sawada, S., and Gilbert, E. (2002) Expression of the palmitoylation-deficient CD151 weakens the association of $\alpha 3\beta 1$ integrin with the tetraspanin-enriched microdomains and affects integrin-dependent signaling. *J. Biol. Chem.* **277,** 36991–37000
20. Iwamoto, R., Mine, N., Kawaguchi, T., Minami, S., Saeki, K., and Mekada, E. (2010) HB-EGF function in cardiac valve development requires interaction with heparan sulfate proteoglycans. *Development* **137,** 2205–2214
21. Takazaki, R., Shishido, Y., Iwamoto, R., and Mekada, E. (2004) Suppression of the biological activities of the epidermal growth factor (EGF)-like domain by the heparin-binding domain of heparin-binding EGF-like growth factor. *J. Biol. Chem.* **279,** 47335–47343
22. Berditchevski, F., and Odintsova, E. (1999) Characterization of integrin-tetraspanin adhesion complexes. Role of tetraspanins in integrin signaling. *J. Cell Biol.* **146,** 477–492
23. Bolte, S., and Cordelières, F. P. (2006) A guided tour into subcellular colocalisation analysis in light microscopy. *J. Microsc.* **224,** 213–232
24. Kleijmeer, M. J., Raposo, G., and Geuze, H. J. (1996) Characterization of MHC class II compartments by immunoelectron microscopy. *Methods* **10,** 191–207
25. Liou, W., Geuze, H. J., and Slot, J. W. (1996) Improving structural integrity of cryosections for immunogold labeling. *Histochem. Cell Biol.* **106,** 41–58
26. Roepstorff, K., Grandal, M. V., Henriksen, L., Knudsen, S. L., Lerdrup, M., Grøvdal, L., Willumsen, B. M., and van Deurs, B. (2009) Differential effects of EGFR ligands on endocytic sorting of the receptor. *Traffic* **10,** 1115–1127
27. Baldys, A., Göoz, M., Morinelli, T. A., Lee, M.-H., Raymond, J. R. Jr., Luttrell, L. M., and Raymond, J. R., Sr. (2009) Essential role of c-Cbl in amphiregulin-induced recycling and signaling of the endogenous epidermal growth factor receptor. *Biochemistry* **48,** 1462–1473
28. Roepstorff, K., Grøvdal, L., Grandal, M., Lerdrup, M., and van Deurs, B. (2008) Endocytic downregulation of ErbB receptors. Mechanisms and relevance in cancer. *Histochem. Cell Biol.* **129,** 563–578
29. Swaminathan, G., and Tsygankov, A. Y. (2006) The Cbl family proteins. Ring leaders in regulation of cell signalling. *J. Cell. Physiol.* **209,** 21–43
30. Pedraza-Alva, G., Sawasdikosol, S., Liu, Y. C., Mérida, L. B., Cruz-Muñoz, M. E., Oceguera-Yañez, F., Burakoff, S. J., and Rosenstein, Y. (2001) Regulation of Cbl molecular interactions by the co-receptor molecule CD43 in human T cells. *J. Biol. Chem.* **276,** 729–737
31. Melander, F., Andersson, T., and Dib, K. (2004) Engagement of $\beta 2$ integrins recruits 14-3-3 proteins to c-Cbl in human neutrofils. *Biochem. Biophys. Res. Commun.* **317,** 1000–1005
32. Zhang, X. A., Bontrager, A. L., and Hemler, M. E. (2001) Transmembrane-4 superfamily proteins associate with activated protein kinase C (PKC) and link PKC to specific β_1 integrins. *J. Biol. Chem.* **276,** 25005–25013
33. Bao, J., Alroy, I., Waterman, H., Schejter, E. D., Brodie, C., Gruenberg, J., and Yarden, Y. (2000) Threonine phosphorylation diverts internalised epidermal growth factor receptors from a degradative pathway to the recycling endosome. *J. Biol. Chem.* **275,** 26178–26186
34. Cotton, C. U., Hobert, M. E., Ryan, S., and Carlin, C. R. (2013) Basolateral EGF receptor sorting regulated by functionally distinct mechanisms in renal epithelial cells. *Traffic* **14,** 337–354
35. Stern, K. A., Place, T. L., and Lill, N. L. (2008) EGF and amphiregulin differentially regulate Cbl recruitment to endosomes and EGF receptor fate. *Biochem. J* **410,** 585–594
36. Forsten-Williams, K., Chu, C. L., Fannon, M., Buczek-Thomas, J. A., and Nugent, M. A. (2008) Control of growth factor networks by heparan sulfate proteoglycans. *Ann. Biomed. Eng.* **36,** 2134–2148
37. Gitay-Goren, H., Soker, S., Vlodavsky, I., and Neufeld, G. (1992) The binding of vascular endothelial growth factor to its receptors is dependent on cell-surface-associated heparin-like molecules. *J. Biol. Chem.* **267,** 6093–6098
38. Higashiyama, S., Abraham, J. A., and Klagsbrun, M. (1993) Heparin-binding EGF-like growth factor stimulation of smooth muscle cell migration. Dependence on interactions with cell surface heparan sulfate. *J. Cell Biol.* **122,** 933–940

39. Mahtouk, K., Cremer, F. W., Rème, T., Jourdan, M., Baudard, M., Moreaux, J., Requirand, G.,Fiol, G., De Vos, J., Moos, M., Quittet, P., Goldschmidt, H., Rossi, J. F., Hose, D., and Klein, B. (2006) Heparan sulfate proteoglycans are essential for the myeloma cell growth activity of EGF-family ligands in multiple myeloma. *Oncogene* **25,** 7180–7191
40. Couchman, J. R. (2010) Transmembrane signalling. Proteoglycans. *Annu. Rev. Cell Dev. Biol.* **26,** 89–114
41. Keum, E., Kim, Y., Kim, J., Kwon, S., Lim, Y., Han, I., and Oh, E.-S. (2004) Syndecan-4 regulates localization, activity and stability of protein kinase C-α. *Biochem. J.* **378,** 1007–1014
42. Fan, T.-C., Chang, H.-T., Chen, I-W., Wang, H.-Y., and Chang, M. D.-T. (2007) A heparan sulfate-facilitated and raft-dependent macropinocytosis of eosinophil cationic protein. *Traffic* **8,** 1778–1795
43. Tkachenko, E., Lutgens, E., Stan, R.-V., and Simons, M. (2004) Fibroblast growth factor 2 endocytosis in endothelial cells proceed via syndecan-4-dpendent macropinocytic pathway. *J. Cell Sci.* **117,** 3189–3199
44. Lambaerts, K., Wilcox-Adelman, S. A., and Zimmermann, P. (2009) The signalling mechanisms of syndecan heparan sulfate proteoglycans. *Curr. Opin. Cell Biol.* **21,** 662–669
45. Clague, M. J., Liu, H., and Urbé, S. (2012) Governance of endocytic trafficking and signaling by reversible ubiquitylation. *Dev. Cell* **23,** 457–467